

This is a provisional PDF only. Copyedited and fully formatted version will be made available soon.

REPORTS OF PRACTICAL ONCOLOGY AND RADIOTHERAPY

ISSN: 1507-1367

e-ISSN: 2083-4640

Verification of stereotactic radiosurgery plans for multiple brain metastases using a virtual phantom-based procedure

Authors: Juan-Francisco Calvo-Ortega, Peter B. Greer, Sandra Moragues-Femenía, Miguel Pozo-Massó, Joan Casals-Farran

DOI: 10.5603/RPOR.a2022.0042

Article type: Research paper

Published online: 2022-03-30

This article has been peer reviewed and published immediately upon acceptance. It is an open access article, which means that it can be downloaded, printed, and distributed freely, provided the work is properly cited.

Verification of stereotactic radiosurgery plans for multiple brain metastases using a virtual phantom-based procedure

10.5603/RPOR.a2022.0042

Juan-Francisco Calvo-Ortega¹, Peter B. Greer², Sandra Moragues-Femenía¹, Miguel Pozo-Massó¹, Joan Casals-Farran¹

¹*Servicio de Oncología Radioterápica, Hospital Quirónsalud Barcelona, Barcelona, Spain*

²*Department of Radiation Oncology, Calvary Mater Newcastle Hospital, Newcastle, Australia*

Correspondence to: Juan-Francisco Calvo-Ortega, Servicio de Oncología Radioterápica, Hospital Quirónsalud Barcelona, Barcelona, Spain; e-mail: jfcdrr@yahoo.es

Abstract

Background: The purpose of this study was to describe the use of the VIPER software for patient-specific quality assurance (PSQA) of single-isocenter multitarget (SIMT) stereotactic radiosurgery (SRS) plans.

Materials and methods: Twenty clinical of intensity-modulated (IMRT) SIMT SRS plans were reviewed. A total of 88 brain metastases were included. Number of lesions per plan and their individual volumes ranged from 2 to 35 and from 0.03 to 32.8 cm³, respectively. Plans were designed with the Eclipse system, and delivered using a Varian CLINAC linac. SRS technique consisted of non-coplanar static-field sliding-window IMRT.

Each plan was mapped onto a virtual cylindrical water phantom (VCP) in the Eclipse to calculate a 3D dose distribution (verification plan). The VIPER software reconstructed the 3D dose distribution inside the VCP from the acquired in-air electronic portal image device (EPID) images of the treatment fields.

A 3D gamma analysis was used to compare the reconstructed doses to the Eclipse planned doses on the VCP. Gamma passing rates (GPRs) were calculated using 3% global/2 mm criteria and dose thresholds ranged from 10% to 90% of the maximum dose.

Results: The averages (± 1 SD) of the 3D GPRs over the 20 SRS plans were: $99.9 \pm 0.2\%$, $99.7 \pm 0.3\%$, $99.6 \pm 0.5\%$, $99.3 \pm 0.9\%$, $99.1 \pm 1.6\%$, $99.0 \pm 1.6\%$, and $98.5 \pm 3.3\%$, for dose thresholds of 10%, 20%, 30%, 50%, 70%, 80% and 90% respectively.

Conclusions: This work shows the feasibility of the VIPER software for PSQA of SIMT SRS plans, being a reliable alternative to commercially available 2D detector arrays.

Key words: EPID; virtual phantom; single-isocenter; SRS

Introduction

The use of stereotactic radiosurgery (SRS) for treatment of multiple brain metastases (BMs) has increased over the last years. Many articles and guidelines have suggested the role of SRS for patients with multiple BMs [1–5]. For instance, the prospective trial of Yamamoto et al. found no differences in overall survival or neurologic mortality with SRS for 2 to 4 versus 5 to 10 BMs [2]. The SRS is preferred over WBRT in limited brain metastases because it has shown better learning and memory preservation in several randomised trials. Moreover, it is emerging as an alternative treatment in selected cases of multiple brain lesions (up to 15) because it did not seem to affect the survival outcome [6].

Delivery of SRS for multiple BMs has been described using the Gamma Knife (GK) treatment unit (Elekta, Stockholm, Sweden), considered by some as the gold standard of treatment in terms of sparing normal tissue and high localization precision [7, 8]. However, a recent multi-institutional study found similar overall survival with lower incidence of radionecrosis in patients with multiple BMs treated with linear accelerators (linac) compared to GK SRS [9]. A single isocenter cannot be used with GK to treat all of the lesions simultaneously at the cost of long beam-on times of even hours [10]. In contrast, linacs do allow the use of a single isocenter such that multiple BMs can be simultaneously treated within several minutes [11]. The use of single isocenter and delivery techniques of intensity-modulated (IMRT) and volumetric arc therapy (VMAT) has expanded in recent years for simultaneous SRS of multiple BMs [12–15].

SRS treatment plans present higher dose heterogeneity and faster dose fall-offs in tissue around the targets in comparison with conventionally fractionated radiotherapy. Clinical implementation of linac-based SRS for multiple BMs requires a patient-specific quality assurance (PSQA) procedure to verify that the approved treatment plan can be accurately delivered. A pre-treatment verification of dose delivery based on dosimetric measurements is highly recommended within the PSQA [16].

To do such measurements, a few “stereotactic” 2D arrays with a relatively high spatial resolution are commercially available. Higher spatial resolution, larger detection area and lack of angular dependence which enable non-coplanar measurements can be attained with a radiochromic film. Although film is typically limited to measurements in either a coronal or sagittal plane, a cylindrical rotational phantom allowing any plane orientation has been described [17]. However, still it is not always possible to catch all targets in a single measurement performed with a 2D detector. Linacs are currently equipped with electronic portal imaging devices (EPIDs) with a large detection area (up to 40 x 40 cm²) and high spatial resolution (up to 0.3 mm/pixel), making possible a three-dimensional (3D) dose reconstruction over the whole patient head volume [18]. Therefore, the EPIDs offer an interesting solution for verification of single isocenter multiple-target (SIMT) SRS plans, if 3D dose reconstruction is performed [19]. This approach was described by Ansbacher for verification of IMRT plans [20]. Audits of IMRT and VMAT for clinical trials have been done using the VIPER (VIrtual Phantom Epid dose Reconstruction) software that permits the 3D dose reconstruction from EPID images [21, 22]. However, no SRS plans were included in those audits.

There are several commercially available systems offering 3D dose reconstruction from EPID-based measurements, but none of them is designed to work using a virtual phantom [23]. Recently, the accuracy of the VIPER software has been assessed by our group to be used for 3D SRS verification [24]. The aim of this study is to describe our experience using the VIPER software for PSQA of SIMT SRS plans.

Materials and methods

The VIPER software

The VIPER software was developed at the Calvary Mater Newcastle Hospital (CMNH) for EPID-based 3D dose distribution reconstruction onto a virtual water phantom

[25, 26]. VIPER can be used for either 2D or 3D dose reconstruction to perform dosimetric verification of the individual fields or composite plan, respectively. However, it was shown by Kruse that single field planar verification is insensitive and not sufficient to detect important dosimetric inaccuracies of the overall IMRT plan [27]. Therefore, 3D reconstructed dose-based verification is better than using 2D reconstructed doses. The resulting 3D dose can be compared with the corresponding dose distribution computed by a treatment planning system (TPS) to be evaluated.

Instructions provided by CMNH were followed to obtain a VIPER (v. 3.10 beta, May 2019) calibration tailored to our facility. VIPER was configured for 6 MV beams from a Varian CLINAC 2100 CD linac (Varian Medical Systems, Palo Alto, CA), equipped with the Millennium 120 multileaf collimator (MLC) and the PortalVision aS500 EPID. Repetition rate of 600 monitor units per minute was used.

The validation and feasibility of VIPER for SRS plan verification were described by our group in a recent publication [24].

Evaluation of SIMT SRS plans using VIPER

At the time of elaboration of this manuscript, SIMT SRS plans were planned in our department with the sliding window IMRT technique, by using a non-coplanar arrangement of 6 MV beams from a CLINAC 2100 CD linac. Plans were calculated with 1 mm grid size using the anisotropic algorithm (AAA) algorithm of the Eclipse TPS. In a previous work, we investigated the Eclipse dose calculation accuracy, as well as the targeting accuracy of our linac to treat multiple targets with a single-isocenter [28, 29].

Figure 1 shows the flux diagram to perform a 3D VIPER-based verification of a SIMT SRS plan. In the Eclipse TPS, the patient plan has to be copied onto a virtual cylindrical phantom (VCP) to be recalculated by keeping the original MUs and fluences (verification plan). Then, the VCP-based plan and an open 10x10 cm² field (100 MU) have to be delivered onto the EPID. The 10 x 10 cm² image is used by VIPER to calibrate the EPID signal to dose conversion, as VIPER cannot assess absolute beam output. Optionally, the EPID image from a 40 x 30 cm² field covering whole detector is used to normalize the off-axis response of the EPID. For all the plans included in this study, 10 x 10 cm² and the 40 x 30 cm² calibration images were acquired on each verification plan. The recorded images in DICOM format, the RP DICOM

Plan file and the RD DICOM Dose files of the SRS plan to be verified are imported into VIPER software. VIPER uses the gantry angle reported in the DICOM image header for its dose reconstruction, and this relies on regular quality assurance of gantry angle as is required in radiation therapy.

VIPER imports the TPS dose matrix and interpolates it to 2 mm isotropic coordinates. VIPER then calculates the 3D dose in VCP from at the same resolution (2 mm). This resolution is a compromise to get reasonable speed and not require too much RAM memory. Both dose distributions are interpolated to a fine grid resolution of 0.8 mm, and the gamma index for each fine grid point is calculated. The conventional gamma index calculation algorithm is used which calculates the absolute magnitude of dose difference [30]. To avoid erroneous gamma normalization doses due to EPID noise, the TPS dose is used as reference. Once the gamma index values are obtained, they are interpolated back to 2 mm resolution. Finally, both dose distributions (Eclipse vs. VIPER) can be compared using the 2D and 3D gamma analysis tools available in the VIPER software (Fig. 2).

Twenty SIMT SRS cases (88 BMs) treated at our department were retrospectively included in this study. The number of lesions per case and their individual volumes ranged from 2 to 35 (median: 2) and 0.03 to 32.8 cm³ (median: 0.7 cm³), respectively. The median distance from the center of each lesion to the treatment isocenter was 5.8 cm (range: 0.3–10.5 cm).

The dosimetric agreement between Eclipse and VIPER plans was assessed using the 3D gamma tool available in the VIPER software. Global gamma analysis was used, i.e., the dose difference is calculated in respect to the maximum dose given by Eclipse. At least 1 mm and 5% dose accuracy is recommended in SRS treatment verification due to the high-spatial resolution and high-accuracy in dose required for this kind of treatment, respectively.³¹

As Miften et al. stated, there is a need to consider both the spatial and dosimetric uncertainties when comparing dose distributions to determine if the reference and evaluated dose distributions agree to within the limits that are clinically relevant [32]. In the gamma index analysis, the spatial analog to the dose difference is the distance-to-agreement (DTA) metric. As the dose distribution measurements have some spatial uncertainty, the DTA criterion can be partly defined based on the measurement error. The mechanical accuracy of the EPID arm during gantry rotation, including the ISOCAL EPID positional correction available on the Varian CLINAC, was assessed in 0.6 mm. Therefore, although SRS delivery

accuracy is aimed for < 1 mm, we have chosen a DTA of 2 mm to take into account the EPID positional error. In the context of PTV margins used for treatment, Bossuyt et al. described the use of the CTV-PTV margin as DTA for transit in-vivo PSQA based on EPID measurements [33]. The 2 mm-DTA used in the present study coincides with the CTV-PTV margin implemented in our SIMT SRS policy [29]. So, a successful GPR using 2 mm-DTA is compatible with an adequate dosimetric coverage of the lesions.

On the other hand, the Task Group (TG) No 218 report of the American Association of Physicists in Medicine (AAPM) recommends the use of 3%/2 mm for patient-specific IMRT QA [32]. So, gamma passing rates (GPRs) using the 3%/2 mm criteria were computed in this study for dose thresholds of 10%, 20%, 30%, 50%, 70%, 80%, and 90% of the maximum dose (100%) computed by the VIPER software. A level of 90% GPR was considered as the minimum acceptable for the comparison.³²

Evaluation of the VIPER sensitivity

The sensitivity of the software VIPER to catch dosimetric errors was evaluated using a SIMT-SRS plan designed in the Eclipse TPS for ten 1 cm-diameter targets scattered inside the VCP (reference plan). This plan was irradiated onto the EPID and the corresponding 3D dose reconstruction was performed with VIPER. 3D gamma analysis with 3%/2 mm criteria was done and the GPRs for the dose thresholds of 10%, 20%, 30%, 50%, 70%, 80%, and 90% were used as references. Three new plans were created in the Eclipse TPS by introducing intentional MLC errors in the reference plan, by shifting all the leaves in the MLC bank A by 0.2, 0.5, and 1 mm, respectively. For each erroneous plan, a VIPER verification was done using the EPID images of the reference plan.

Results

The 3D dose distributions computed in the VCP by the Eclipse TPS were compared with those given by the VIPER software. Table 1 summarizes the 3D gamma analysis results for criteria of 3%/2 mm and different threshold values of the maximum dose in the VCP, for the twenty SIMT SRS cases included in this study. Average 3D GPRs were greater than 98% for all threshold values. The minimum GPR was 86.9% and it was registered for the 90% dose threshold. For the remaining dose thresholds, all GPRs were above the 90% acceptability limit. Confidence limits (CLs), as baseline expectation values for QA of SIMT

SRS plans, were calculated following the methodology described by the AAPM TG-119.³⁴ Figure 3 illustrates the 3D GPRs.

Figure 4 shows the sensitivity of the VIPER software to the intentionally created dosimetric errors in the MLC. The 3D GPRs for 3%/2 mm criteria decreased with the induced errors for all dose thresholds used for the gamma analysis. However, the dose thresholds detecting a GPR below the acceptable limit of 90% were 90%, 50% and 20% for the 0.2, 0.5 and 1 mm induced errors, respectively.

Discussion

We have previously reported the accuracy of the VIPER software to be used for PSQA of SIMT SRS plans [24]. In the current study its application for verification of clinical plans designed with the Eclipse TPS has been described.

The 3D gamma analysis over the 20 SIMRT SRS plans showed excellent GPRs, regardless of the applied dose threshold (Tab. 1). A reduction of the mean GPR and an increment of SD of GPR were observed as the dose threshold decreased, as the number of voxels contained in the dose threshold-defined volume decreases. Anyway, very high CLs for the GPR were obtained for all dose thresholds. For the 90% dose threshold, the CL was 92%, i.e., still above the universal action limits recommended by the AAPM TG-218 report [32]. Prescription dose is typically assigned to the 70–80% isodose line in our SRS plans, being 100% the maximum dose. Therefore, the 3D gamma analysis in the region of the VCP confined by the 90% dose threshold may not be too significant for our analysis. On the other hand, VIPER was sensitive to detect a MLC error of 1 mm when a dose threshold of at least 20% was used. Therefore, we look at the 3%/2 mm GPRs for thresholds from 20% to 80% when SIMT SRS plans are verified using the VIPER software.

The sensitivity test reported that the smaller induced error of 0.2 mm could be caught by VIPER when the 90%-threshold is inspected. So, VIPER is able to detect systematic errors in leaf position below the 0.3–0.5 mm limit required to ensure acceptable levels of deviation in dose [35, 36].

The VIPER software is a virtual non-transit 3D dosimetry method, alternative to the use of physical phantoms. The literature available about this method for verification of SIMT

SRS plan is scarce. Olaciregui-Ruiz et al. compared the planned with the reconstructed dose distributions generated using a research version of the iViewDose system (Elekta AB, Stockholm, Sweden) [37]. They performed 3D gamma analysis (3% global/2 mm) within the volume surrounded by the isodose surface defined by 50% of the maximum planned dose, with an average GPR of $98.0 \pm 3.0\%$, but verifications of SIMT SRS plans were not included. Alhazmi et al. also described the feasibility of verified IMRT and VMAT plans using an EPID-based algorithm for 3D dose reconstruction on a virtual cylindrical water phantom, but SIMT SRS plans were not included in their study [38].

As far as we know, our study is the first application of non-transit 3D EPID dosimetry for pre-treatment PSQA of SIMT SRS plans. This study reveals the VIPER software as an excellent tool for verification of SIMT plans, without the pitfalls related to the detector size and spatial resolution of commercially available 2D detectors.

Several limitations of the version of the VIPER software used in this study can be mentioned:

1. This study does not include VMAT plans, as this technology was not available at our department. However, we truly expect that the outcomes achieved in this work can be extend for VMAT SRS plans. This issue will be investigated by our group in the near future;
2. VIPER uses in air-EPID images to reconstruct the 3D dose inside a virtual phantom. So, potential dosimetric errors due to inaccuracy of the linac couch rotation will not be always detected by VIPER. This is a VIPER drawback in comparison with commercially available 2D detector arrays, which may have worse detector resolution but when placed on the couch they can verify overall effect of all components of a treatment plan. In this way, VIPER is able to detect discrepancies between the planned and the actual beam delivery onto a virtual cylindrical water phantom, excluding the potential couch rotation inaccuracy. This issue has to be controlled using an additional check, as for instance the Winston-Lutz test that we perform in our clinical practice [39];
3. Rodriguez et al. defined a metric named dose-volume histogram (DVH) percentage of agreement (PA), and showed that it was more sensitive than GPR to detect dosimetric errors [40]. DVH calculation, however, is not currently available in the VIPER software. The implementation of a DVH approach in the VIPER software was also proposed by Miri et al. [22];

4. 3D dose distribution reconstruction on the patient's CT anatomy cannot be done by the VIPER software, as it is currently performed by other commercially-available systems [41, 42];

5. As pointed out by Miri et al. [22], VIPER does not allow an end-to-end audit to be performed, for instance, absolute beam output, beam profile or inhomogeneity modelling cannot be assessed.

Conclusions

This work shows the feasibility of the VIPER software for patient-specific QA of single-isocenter multiple-target SRS plans, being a reliable alternative to commercially available 2D detector arrays for this task.

Acknowledgments

The authors would like to thank Dr J. Scherman for the assistance he provided in designing the intended errors in the original MLC patterns used in this study, and Dr M. Hermida-López for the suggestions and comments he provided.

Dedicated to the memory of Dr A. Feixa, who sadly passed away due to the COVID-19 pandemic.

Conflict of interests

None declared.

Funding

None declared.

References

1. ¹ Bhatnagar AK, Kondziolka D, Lunsford LD, et al. Stereotactic radiosurgery for four or more intracranial metastases. *Int J Radiat Oncol Biol Phys.* 2006; 64(3): 898-903, doi: [10.1016/j.ijrobp.2005.08.035](https://doi.org/10.1016/j.ijrobp.2005.08.035), indexed in Pubmed: [16338097](https://pubmed.ncbi.nlm.nih.gov/16338097/).

2. Yamamoto M, Serizawa T, Higuchi Y, et al. Stereotactic radiosurgery for patients with multiple brain metastases (JLGK0901): a multi-institutional prospective observational study. *Lancet Oncol.* 2014; 15(4): 387-395, doi: [10.1016/S1470-2045\(14\)70061-0](https://doi.org/10.1016/S1470-2045(14)70061-0), indexed in Pubmed: [24621620](https://pubmed.ncbi.nlm.nih.gov/24621620/).
3. Limon D, McSherry F, Herndon J, et al. Single fraction stereotactic radiosurgery for multiple brain metastases. *Adv Radiat Oncol.* 2017; 2(4): 555-563, doi: [10.1016/j.adro.2017.09.002](https://doi.org/10.1016/j.adro.2017.09.002), indexed in Pubmed: [29204522](https://pubmed.ncbi.nlm.nih.gov/29204522/).
4. Niranjana A, Monaco E, Flickinger J, et al. Guidelines for Multiple Brain Metastases Radiosurgery. *Prog Neurol Surg.* 2019; 34: 100-109, doi: [10.1159/000493055](https://doi.org/10.1159/000493055), indexed in Pubmed: [31096242](https://pubmed.ncbi.nlm.nih.gov/31096242/).
5. Kraft J, Zindler J, Minniti G, et al. Stereotactic Radiosurgery for Multiple Brain Metastases. *Curr Treat Options Neurol.* 2019; 21(2): 6, doi: [10.1007/s11940-019-0548-3](https://doi.org/10.1007/s11940-019-0548-3), indexed in Pubmed: [30758726](https://pubmed.ncbi.nlm.nih.gov/30758726/).
6. Hughes RT, Masters AH, McTyre ER, et al. Initial SRS for Patients With 5 to 15 Brain Metastases: Results of a Multi-Institutional Experience. *Int J Radiat Oncol Biol Phys.* 2019; 104(5): 1091-1098, doi: [10.1016/j.ijrobp.2019.03.052](https://doi.org/10.1016/j.ijrobp.2019.03.052), indexed in Pubmed: [30959122](https://pubmed.ncbi.nlm.nih.gov/30959122/).
7. Semwal MK, Singh S, Sarin A, et al. Comparative clinical dosimetry with X-knife and gamma knife. *Phys Med.* 2012; 28(3): 269-272, doi: [10.1016/j.ejmp.2011.07.003](https://doi.org/10.1016/j.ejmp.2011.07.003), indexed in Pubmed: [21803627](https://pubmed.ncbi.nlm.nih.gov/21803627/).
8. McDonald D, Schuler J, Takacs I, et al. Comparison of radiation dose spillage from the Gamma Knife Perfexion with that from volumetric modulated arc radiosurgery during treatment of multiple brain metastases in a single fraction. *J Neurosurg.* 2014; 121 Suppl: 51-59, doi: [10.3171/2014.7.GKS141358](https://doi.org/10.3171/2014.7.GKS141358), indexed in Pubmed: [25434937](https://pubmed.ncbi.nlm.nih.gov/25434937/).
9. Sebastian NT, Glenn C, Hughes R, et al. Linear accelerator-based radiosurgery is associated with lower incidence of radionecrosis compared with gamma knife for treatment of multiple brain metastases. *Radiother Oncol.* 2020; 147: 136-143, doi: [10.1016/j.radonc.2020.03.024](https://doi.org/10.1016/j.radonc.2020.03.024), indexed in Pubmed: [32294607](https://pubmed.ncbi.nlm.nih.gov/32294607/).
10. Vergalaso I, Liu H, Alonso-Basanta M, et al. Multi-Institutional Dosimetric Evaluation of Modern Day Stereotactic Radiosurgery (SRS) Treatment Options for Multiple Brain Metastases. *Front Oncol.* 2019; 9: 483, doi: [10.3389/fonc.2019.00483](https://doi.org/10.3389/fonc.2019.00483), indexed in Pubmed: [31231614](https://pubmed.ncbi.nlm.nih.gov/31231614/).
11. Ma L, Nichol A, Hossain S, et al. Variable dose interplay effects across radiosurgical apparatus in treating multiple brain metastases. *Int J Comput Assist Radiol Surg.* 2014; 9(6): 1079-1086, doi: [10.1007/s11548-014-1001-4](https://doi.org/10.1007/s11548-014-1001-4), indexed in Pubmed: [24748208](https://pubmed.ncbi.nlm.nih.gov/24748208/).
12. Nath SK, Lawson JD, Simpson DR, et al. Single-isocenter frameless intensity-modulated stereotactic radiosurgery for simultaneous treatment of multiple brain metastases: clinical experience. *Int J Radiat Oncol Biol Phys.* 2010; 78(1): 91-97, doi: [10.1016/j.ijrobp.2009.07.1726](https://doi.org/10.1016/j.ijrobp.2009.07.1726), indexed in Pubmed: [20096509](https://pubmed.ncbi.nlm.nih.gov/20096509/).
13. Audet C, Poffenbarger BA, Chang P, et al. Evaluation of volumetric modulated arc therapy for cranial radiosurgery using multiple noncoplanar arcs. *Med Phys.* 2011; 38(11): 5863-5872, doi: [10.1118/1.3641874](https://doi.org/10.1118/1.3641874), indexed in Pubmed: [22047350](https://pubmed.ncbi.nlm.nih.gov/22047350/).
14. Lawson JD, Wang JZ, Nath SK, et al. Intracranial application of IMRT based radiosurgery to treat multiple or large irregular lesions and verification of infra-red frameless localization system. *J Neurooncol.* 2010; 97(1): 59-66, doi: [10.1007/s11060-009-9987-0](https://doi.org/10.1007/s11060-009-9987-0), indexed in Pubmed: [19693438](https://pubmed.ncbi.nlm.nih.gov/19693438/).

15. Thomas EM, Popple RA, Wu X, et al. Comparison of plan quality and delivery time between volumetric arc therapy (RapidArc) and Gamma Knife radiosurgery for multiple cranial metastases. *Neurosurgery*. 2014; 75(4): 409–17; discussion 417, doi: [10.1227/NEU.0000000000000448](https://doi.org/10.1227/NEU.0000000000000448), indexed in Pubmed: [24871143](https://pubmed.ncbi.nlm.nih.gov/24871143/).
16. Hartgerink D, Swinnen A, Roberge D, et al. LINAC based stereotactic radiosurgery for multiple brain metastases: guidance for clinical implementation. *Acta Oncol*. 2019; 58(9): 1275–1282, doi: [10.1080/0284186X.2019.1633016](https://doi.org/10.1080/0284186X.2019.1633016), indexed in Pubmed: [31257960](https://pubmed.ncbi.nlm.nih.gov/31257960/).
17. Grams MP, de Los Santos LE. Design and clinical use of a rotational phantom for dosimetric verification of IMRT/VMAT treatments. *Phys Med*. 2018; 50: 59–65, doi: [10.1016/j.ejmp.2018.05.019](https://doi.org/10.1016/j.ejmp.2018.05.019), indexed in Pubmed: [29891095](https://pubmed.ncbi.nlm.nih.gov/29891095/).
18. Varian manual. “TrueBeam Technical Reference Guide – Volume 2: Imaging, P1005924-001-A”.
19. Ahmed S, Kapatoes J, Zhang G, et al. A hybrid volumetric dose verification method for single-isocenter multiple-target cranial SRS. *J Appl Clin Med Phys*. 2018; 19(5): 651–658, doi: [10.1002/acm2.12430](https://doi.org/10.1002/acm2.12430), indexed in Pubmed: [30112817](https://pubmed.ncbi.nlm.nih.gov/30112817/).
20. Ansbacher W. Three-dimensional portal image-based dose reconstruction in a virtual phantom for rapid evaluation of IMRT plans. *Med Phys*. 2006; 33(9): 3369–3382, doi: [10.1118/1.2241997](https://doi.org/10.1118/1.2241997), indexed in Pubmed: [17022233](https://pubmed.ncbi.nlm.nih.gov/17022233/).
21. Miri N, Lehmann J, Legge K, et al. Virtual EPID standard phantom audit (VESPA) for remote IMRT and VMAT credentialing. *Phys Med Biol*. 2017; 62(11): 4293–4299, doi: [10.1088/1361-6560/aa63df](https://doi.org/10.1088/1361-6560/aa63df), indexed in Pubmed: [28248642](https://pubmed.ncbi.nlm.nih.gov/28248642/).
22. Miri N, Legge K, Colyvas K, et al. A remote EPID-based dosimetric TPS-planned audit of centers for clinical trials: outcomes and analysis of contributing factors. *Radiat Oncol*. 2018; 13(1): 178, doi: [10.1186/s13014-018-1125-8](https://doi.org/10.1186/s13014-018-1125-8), indexed in Pubmed: [30223857](https://pubmed.ncbi.nlm.nih.gov/30223857/).
23. Olaciregui-Ruiz I, Beddar S, Greer P, et al. In vivo dosimetry in external beam photon radiotherapy: Requirements and future directions for research, development, and clinical practice. *Phys Imaging Radiat Oncol*. 2020; 15: 108–116, doi: [10.1016/j.phro.2020.08.003](https://doi.org/10.1016/j.phro.2020.08.003), indexed in Pubmed: [33458335](https://pubmed.ncbi.nlm.nih.gov/33458335/).
24. Calvo-Ortega JF, Greer PB, Hermida-López M, et al. Validation of virtual water phantom software for pre-treatment verification of single-isocenter multiple-target stereotactic radiosurgery. *J Appl Clin Med Phys*. 2021; 22(6): 241–252, doi: [10.1002/acm2.13269](https://doi.org/10.1002/acm2.13269), indexed in Pubmed: [34028955](https://pubmed.ncbi.nlm.nih.gov/34028955/).
25. Miri N, Lehmann J, Legge K, et al. Remote dosimetric auditing for intensity modulated radiotherapy: A pilot study. *Phys Imaging Radiat Oncol*. 2017; 4: 26–31, doi: [10.1016/j.phro.2017.11.004](https://doi.org/10.1016/j.phro.2017.11.004).
26. King BW, Morf D, Greer PB. Development and testing of an improved dosimetry system using a backscatter shielded electronic portal imaging device. *Med Phys*. 2012; 39(5): 2839–2847, doi: [10.1118/1.4709602](https://doi.org/10.1118/1.4709602), indexed in Pubmed: [22559656](https://pubmed.ncbi.nlm.nih.gov/22559656/).
27. Kruse JJ. On the insensitivity of single field planar dosimetry to IMRT inaccuracies. *Med Phys*. 2010; 37(6): 2516–2524, doi: [10.1118/1.3425781](https://doi.org/10.1118/1.3425781), indexed in Pubmed: [20632563](https://pubmed.ncbi.nlm.nih.gov/20632563/).
28. Calvo Ortega JF, Moragues S, Pozo M, et al. A dosimetric evaluation of the Eclipse AAA algorithm and Millennium 120 MLC for cranial intensity-modulated radiosurgery. *Med Dosim*. 2014; 39(2): 129–133, doi: [10.1016/j.meddos.2013.11.003](https://doi.org/10.1016/j.meddos.2013.11.003), indexed in Pubmed: [24342166](https://pubmed.ncbi.nlm.nih.gov/24342166/).

29. Calvo-Ortega JF, Pozo M, Moragues S, et al. Targeting accuracy of single-isocenter intensity-modulated radiosurgery for multiple lesions. *Med Dosim.* 2017; 42(2): 104–110, doi: [10.1016/j.meddos.2017.01.006](https://doi.org/10.1016/j.meddos.2017.01.006), indexed in Pubmed: [28478867](https://pubmed.ncbi.nlm.nih.gov/28478867/).
30. Low DA, Harms WB, Mutic S, et al. A technique for the quantitative evaluation of dose distributions. *Med Phys.* 1998; 25(5): 656–661, doi: [10.1118/1.598248](https://doi.org/10.1118/1.598248), indexed in Pubmed: [9608475](https://pubmed.ncbi.nlm.nih.gov/9608475/).
31. Process Management and Quality Assurance for Intracranial Stereotactic Treatment. NEDERLANDSE COMMISSIE VOOR STRALINGSDOSIMETRIE Report 25 of the Netherlands Commission on Radiation Dosimetry October 2015.
32. Miften M, Olch A, Mihailidis D, et al. Tolerance limits and methodologies for IMRT measurement-based verification QA: Recommendations of AAPM Task Group No. 218. *Med Phys.* 2018; 45(4): e53–e83, doi: [10.1002/mp.12810](https://doi.org/10.1002/mp.12810), indexed in Pubmed: [29443390](https://pubmed.ncbi.nlm.nih.gov/29443390/).
33. Bossuyt E, Weytjens R, Nevens D, et al. Evaluation of automated pre-treatment and transit in-vivo dosimetry in radiotherapy using empirically determined parameters. *Phys Imaging Radiat Oncol.* 2020; 16: 113–129, doi: [10.1016/j.phro.2020.09.011](https://doi.org/10.1016/j.phro.2020.09.011), indexed in Pubmed: [33458354](https://pubmed.ncbi.nlm.nih.gov/33458354/).
34. Ezzell GA, Burmeister JW, Dogan N, et al. IMRT commissioning: multiple institution planning and dosimetry comparisons, a report from AAPM Task Group 119. *Med Phys.* 2009; 36(11): 5359–5373, doi: [10.1118/1.3238104](https://doi.org/10.1118/1.3238104), indexed in Pubmed: [19994544](https://pubmed.ncbi.nlm.nih.gov/19994544/).
35. Rangel A, Dunscombe P. Tolerances on MLC leaf position accuracy for IMRT delivery with a dynamic MLC. *Med Phys.* 2009; 36(7): 3304–3309, doi: [10.1118/1.3134244](https://doi.org/10.1118/1.3134244), indexed in Pubmed: [19673226](https://pubmed.ncbi.nlm.nih.gov/19673226/).
36. Rangel A, Dunscombe P. Poster - Thurs Eve-07: The dosimetric consequences of MLC position inaccuracy in IMRT. *Med Phys.* 2008; 35(7Part2): 3402–3403, doi: [10.1118/1.2965926](https://doi.org/10.1118/1.2965926), indexed in Pubmed: [28512816](https://pubmed.ncbi.nlm.nih.gov/28512816/).
37. Olaciregui-Ruiz I, Vivas-Maiques B, Kaas J, et al. Transit and non-transit 3D EPID dosimetry versus detector arrays for patient specific QA. *J Appl Clin Med Phys.* 2019; 20(6): 79–90, doi: [10.1002/acm2.12610](https://doi.org/10.1002/acm2.12610), indexed in Pubmed: [31083776](https://pubmed.ncbi.nlm.nih.gov/31083776/).
38. Alhazmi A, Gianoli C, Neppi S, et al. A novel approach to EPID-based 3D volumetric dosimetry for IMRT and VMAT QA. *Phys Med Biol.* 2018; 63(11): 115002, doi: [10.1088/1361-6560/aac1a6](https://doi.org/10.1088/1361-6560/aac1a6), indexed in Pubmed: [29714714](https://pubmed.ncbi.nlm.nih.gov/29714714/).
39. Calvo-Ortega JF, Moragues-Femenía S, Laosa-Bello C, et al. A closer look at the conventional Winston-Lutz test: Analysis in terms of dose. *Rep Pract Oncol Radiother.* 2019; 24(5): 421–427, doi: [10.1016/j.rpor.2019.07.003](https://doi.org/10.1016/j.rpor.2019.07.003), indexed in Pubmed: [31367194](https://pubmed.ncbi.nlm.nih.gov/31367194/).
40. Rodriguez M, Brualla L. Treatment verification using Varian's dynalog files in the Monte Carlo system PRIMO. *Radiat Oncol.* 2019; 14(1): 67, doi: [10.1186/s13014-019-1269-1](https://doi.org/10.1186/s13014-019-1269-1), indexed in Pubmed: [31014356](https://pubmed.ncbi.nlm.nih.gov/31014356/).
41. Nakaguchi Y, Oono T, Maruyama M, et al. Commissioning and validation of fluence-based 3D VMAT dose reconstruction system using new transmission detector. *Radiol Phys Technol.* 2018; 11(2): 165–173, doi: [10.1007/s12194-018-0451-8](https://doi.org/10.1007/s12194-018-0451-8), indexed in Pubmed: [29532322](https://pubmed.ncbi.nlm.nih.gov/29532322/).
42. Ahn KH, Yenice KM, Koshy M, et al. Frame-based radiosurgery of multiple metastases using single-isocenter volumetric modulated arc therapy technique. *J Appl Clin Med Phys.* 2019; 20(8): 21–28, doi: [10.1002/acm2.12672](https://doi.org/10.1002/acm2.12672), indexed in Pubmed: [31328368](https://pubmed.ncbi.nlm.nih.gov/31328368/).

Figure 1. Workflow for a VIPER verification of a single-isocenter multitarget stereotactic radiosurgery (SIMT SRS) plan. TPS — treatment planning system; CT — computed tomography; VCP — virtual cylindrical water phantom

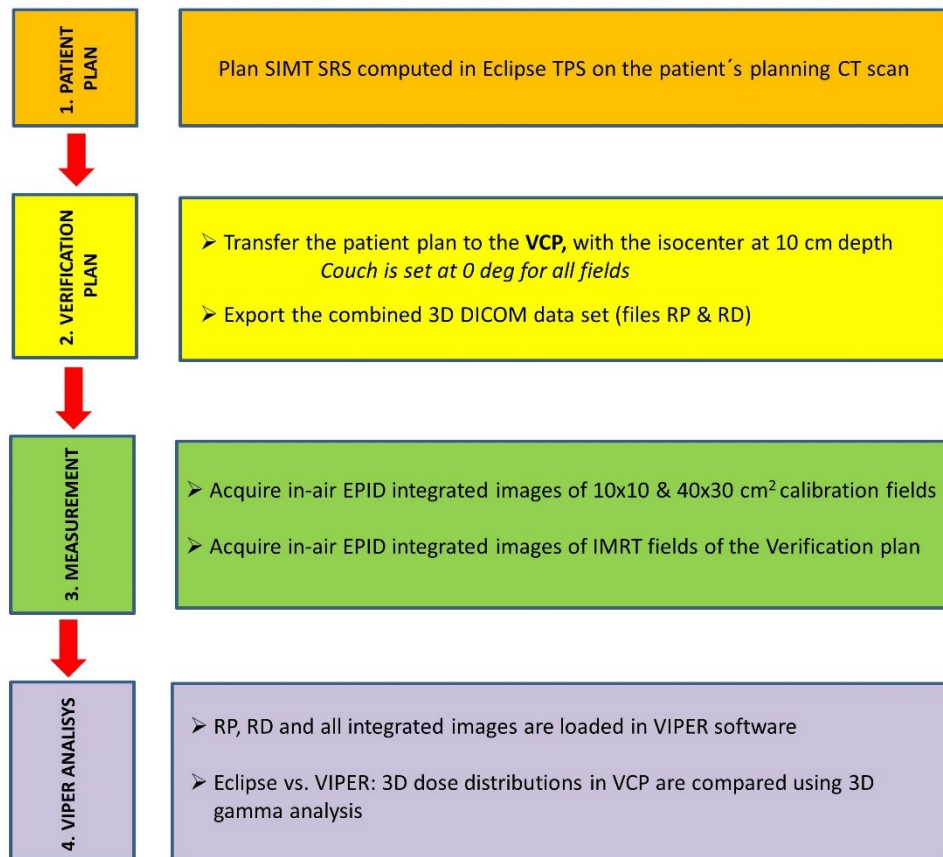


Figure 2. User interface of the VIPER software: the 3D dose distribution from Eclipse (TPS Dose) over the cylindrical water phantom is compared with the corresponding 3D dose derived by VIPER (EPID Dose) from in air EPID-images. The user can synchronically navigate to sagittal, coronal and transversal planes, to compare dose profiles and obtain the 2D gamma index. 3D gamma index is also available

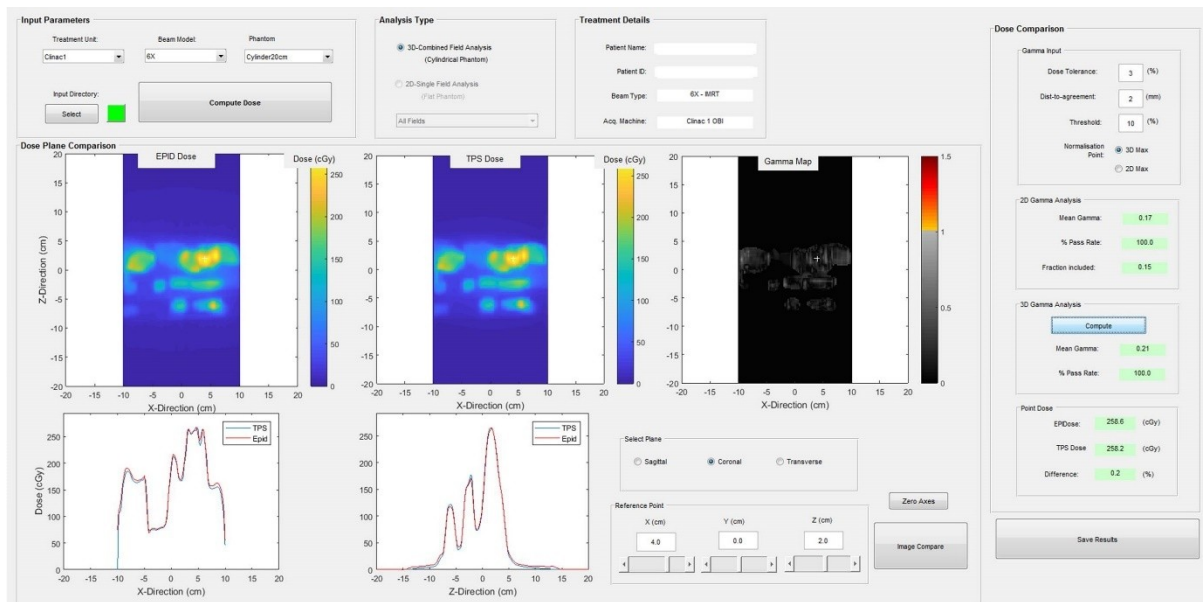


Figure 3. 3D gamma passing rates (GPRs) for VIPER verification of 20 single-isocenter multitarget stereotactic radiosurgery (SIMT SRS) plans calculated in the Eclipse treatment planning system (TPS). Box plots are displayed for several dose thresholds applied in the gamma analysis. Circle: mean; cross: maximum and minimum; box: 25–75% percentiles; whiskers: 5–95% range

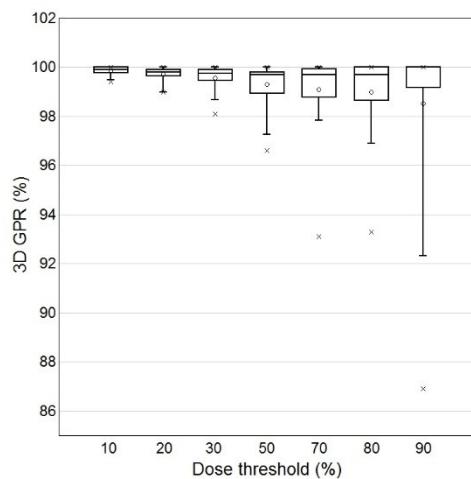


Figure 4. Sensitivity of the gamma passing rates (GPR) metric given by the VIPER software to induced multileaf collimator (MLC) errors of 0.2, 0.5 and 2 mm

